Online and Offline Rotary Regression Analysis of Torque Estimator for Switched Reluctance Motor Drives

X. D. Xue, K. W. E. Cheng, *Senior Member, IEEE*, and S. L. Ho

***Abstract*—A new torque estimator for switched reluctance motor (SRM) drives based on 2-D rotary regression analysis is presented in this paper. The proposed torque estimator is composed of a bicubic regressive polynomial as a function of rotor position and input current. The regressive coefficients can be computed offline or online from the torque characteristics acquired either experimentally or from numerical computation. Furthermore, a torque estimation method by taking mutual coupling into consideration is proposed. It can be seen that the estimated and experimentally obtained self-coupling and mutual-coupling torque characteristics are in good agreement with each other. In addition, the dynamic torque waveforms with and without the mutual coupling, estimated by the proposed estimator, are found to be virtually the same as those obtained from the bicubic spline interpolation for SRM drives with single-pulse voltage, hysteresis current chopping, as well as with voltage pulse width modulation control. The success of all the case studies being reported is a good validation of the usefulness and accuracy of the proposed real-time torque estimator that, as described in this paper, can be used to quickly estimate the instantaneous output torque of SRM drives.**

***Index Terms*—Mutual coupling, regression analysis, switched reluctance motor (SRM), torque estimator.**

NOMENCLATURE

$\boldsymbol{A}$	Information matrix.
I	Phase current.
i_j	Current in phase j.
i_k	Current in phase k.
$I_{\max}$	Maximum current
$I_{\min}$	Minimum current.
N	Number of given torque values.
R	Regressive coefficients matrix, which includes $r_0, r_1, r_2, r_{11}, r_{12}, r_{22}, r_{111}, r_{112}, r_{211}$, and r_{222}.
T_e	Estimated torque.
T_g	Matrix of given torque.
T_k	Instantaneous torque generated by phase k.
T_{km}	Instantaneous mutual-coupling torque generated by the phase adjacent to phase k.
T_{ks}	Instantaneous self-coupling torque from phase k.
W'_{kj}	Mutual-coupling co-energy in phase k generated by the current in phase j that is adjacent to phase k.
W'_{kk}	Self-coupling co-energy generated by the current in phase k.
X	Regressors' matrix that includes x_1, which corresponds to the rotor position, and x_2, which corresponds to the motor current.
μ_2	Regressive parameter corresponding to the second-order regressors.
μ_4	Regressive parameter corresponding to the fourth-order regressors.
μ_6	Regressive parameter corresponding to the sixth-order regressors.
θ	Rotor position.
$\theta_{\max}$	Maximum value of rotor position.
$\theta_{\min}$	Minimum value of rotor position.
ψ_{kj}	Given mutual-coupling flux linkage in phase k generated by the current in phase j that is adjacent to phase k.
ψ_{kk}	Given self-coupling flux linkage characteristics in phase k, which is generated by the current in phase k.

Manuscript received May 11, 2006; revised September 18, 2006. This work was supported by the Research Committee of the Hong Kong Polytechnic University under Project Code G-YX52. Paper no. TEC-00147-2006.

The authors are with the Department of Electrical Engineering, Hong Kong Polytechnic University, Kowloon, Hong Kong (e-mail: eexdxue@polyu.edu.hk; eeecheng@polyu.edu.hk; eeslho@polyu.edu.hk).

Digital Object Identifier 10.1109/TEC.2007.895862

I. INTRODUCTION

A SWITCHED reluctance motor (SRM) has salient poles on both stator and rotor. The windings on the stator have a particularly simple form and there are no windings on the rotor. Thus, the salient advantages of SRM drives are their simple and robust configuration, low rotor inertia, high power-to-volume ratio, high reliability, and low cost. On the other hand, the doubly saliency structure means the air-gap reluctance between the stator and rotor is dependent on the rotor position, and hence, there is inherently more "ripple" in the motor torque. Furthermore, SRM drives need to operate with heavy magnetic saturation in order to obtain good performance. Consequently, both the torque and magnetic characteristics of the motor with respect to the rotor position and the current are highly nonlinear.

Because of the inherent characteristics of SRM drives, the torque ripple minimization study is becoming a topical research area for SRM drives. However, most control strategies incorporating torque ripple minimization need to estimate the instantaneous torque from the rotor position and current in real time [1]. Therefore, the nonlinear torque characteristics at arbitrary rotor positions and currents must be estimated accurately and quickly using a minimal amount of stored data. The present paper is focused on this issue.

Reported torque estimators mainly include four kinds of methodologies, which are, namely, the lookup table approach [2], interpolation [3], analytical approach [4]–[6], and artificial neural network (ANN) [7]. For torque estimators based on the lookup table approach, a set of discrete static torque characteristics are stored in a tabular form, and the instantaneous torque is looked up from the rotor position and the current in real time. However, such torque estimators need to store large amounts of data, and hence, a lot of CPU time is required. For torque estimators based on the interpolation approach, the bicubic spline interpolation is, generally, used to interpolate the torque values from rotor position and motor current. The interpolation coefficients can be computed offline from given static torque characteristics. Torque estimators based on the interpolation approach also require a lot of computation time. Torque estimators based on ANN approach use ANN models to compute the instantaneous torque from the rotor position and the current in real time. However, ANN models have to be trained by using large amounts of given static torque characteristics offline, and the amount of training data strongly affects the accuracy of the ANN estimators. For torque estimators based on the analytical approach, the instantaneous torque is computed by using analytical expressions in which the coefficients are determined offline from the static torque characteristics measured earlier, and hence, the instantaneous torque can be estimated quickly in real time. The accuracy and speed of these torque estimators are dependent on the selected analytical expressions.

In [4], the instantaneous torque is estimated analytically from the flux linkage and air-gap reluctance. However, the flux linkage is estimated from rotor position and motor current using complicated analytical expressions with compound exponent function, and the air-gap reluctance is computed using Fourier series. Clearly, such a torque estimator requires complicated computation and consumes a lot of computation time. An analytical torque estimator is also proposed in [5]. It comprises complicated analytical expression including the square term of the Fourier series, the first-order derivation term of the Fourier series, and the compound exponent term of the Fourier series. This torque estimator, thus, needs complicated computation and computation time. In [6], an analytical torque estimator is presented. It is a complicated analytical expression, which includes the fifth-order polynomials, the compound exponent functions with the fifth-order polynomial, as well as the square term of the fifth-order polynomial. Therefore, the torque estimator proposed in [6] has to process complicated computation and requires substantial computation time.

This study presents a new torque estimator for SRM drives based on rotary regression technique. The 2-D bicubic regressive polynomial is used to model the self-coupling or mutual-coupling torque characteristics. The regressive coefficients in the estimator can be determined either offline or online using the rotary regression scheme. The proposed simple torque estimator only consists of a bicubic polynomial. Hence, it only needs to execute simple computation, stores a small number of given data, and hence, requires a short computation time. The estimated results and the given data are reported to validate the proposed torque estimator.

II. Torque Estimation Technique

A. Torque Estimator

The proposed torque estimator is defined by

$$T_e = \boldsymbol{R}^t \boldsymbol{X} \tag{1}$$

$$\boldsymbol{R} = \begin{pmatrix} r_0 \\ r_{11} \\ r_{22} \\ r_{12} \\ r_1 \\ r_{111} \\ r_{122} \\ r_2 \\ r_{222} \\ r_{211} \end{pmatrix} \tag{2}$$

$$\boldsymbol{X} = \begin{pmatrix} 1 \\ x_1^2 \\ x_2^2 \\ x_1 x_2 \\ x_1 \\ x_1^3 \\ x_1 x_2^2 \\ x_2 \\ x_2^3 \\ x_2 x_1^2 \end{pmatrix} \tag{3}$$

where $\boldsymbol{R}$ denotes the regressive coefficients matrix; $\boldsymbol{R}^t$ denotes the transposed matrix of $\boldsymbol{R}$; T_e denotes the estimated self-coupling or mutual-coupling torque; $r_0, r_{11}, r_{22}, r_{12}, r_1$, $r_{111}, r_{122}, r_2, r_{222}$, and r_{211} are the regressive coefficients determined by the rotary regression scheme, as described in the next section; $\boldsymbol{X}$ denotes the regressors matrix; x_1 and x_2 denote the regressors, which correspond, respectively, to the rotor position and motor current.

The regressor x_1 is computed from

$$\begin{cases} \theta_{\text{av}} = (\theta_{\min} + \theta_{\max})/2 \\ \Delta_\theta = (\theta_{\max} - \theta_{\min})/2 \\ x_1 = (\theta - \theta_{\text{av}})/\Delta_\theta. \end{cases} \tag{4}$$

Similarly, x_2 is determined by

$$\begin{cases} I_{\text{av}} = (I_{\min} + I_{\max})/2 \\ \Delta_I = (I_{\max} - I_{\min})/2 \\ x_2 = (I - I_{\text{av}})/\Delta_I \end{cases} \tag{5}$$

where θ denotes the rotor position, $\theta_{\min}$ denotes the minimum value of the rotor position, $\theta_{\max}$ denotes the maximum value of the rotor position, I is the current, $I_{\min}$ is the minimum current, and $I_{\max}$ is the maximum current. Clearly, x_j satisfies $-1 \le x_j \le 1 (j = 1, 2)$.

It can be seen that the proposed torque estimator is composed of a bicubic polynomial. Hence, it will execute simple computations only, and requires short computation time. In addition, the

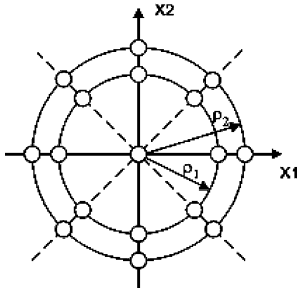

Fig. 1. Schematic diagram of distribution of given points for a rotary regressive scheme.

regressive analysis technique being described in the next section can ensure that the given self-coupling or mutual-coupling torque characteristics can be modeled by the proposed torque estimator accurately.

B. Rotary Regression Scheme

Suppose that N torque values and N pairs of regressors $(x_{l1}, x_{l2}, l = 1, \ldots, N)$ are given in the rotary regression scheme, then the information matrix $\boldsymbol{A}$ is defined by

$$\boldsymbol{A} = \boldsymbol{Y}^t \boldsymbol{Y} \tag{6}$$

where $\boldsymbol{Y}^t$ is the transposed matrix of the matrix $\boldsymbol{Y}$, which only depends on the regressor values and can be expressed by (7) shown at the bottom of the page. It can be observed from (6) and (7) that $\boldsymbol{A}$ is a symmetrical matrix. For a bicubic rotation regression with two regressors, the total given points, except the centric point $(x_1 = x_2 = 0)$, must be located on two or more homocentric circles with different radii, which are not equal to zero. Furthermore, the number of the given points on each circle must be greater than 7, and these points are distributed symmetrically, as shown in Fig. 1. However, the amounts of the given points on each circle may be different, and the amount of the centric points can be selected arbitrarily [8].

Thus, such a rotary regression scheme gives rise to

$$\begin{cases} \sum_{l=1}^{N} x_{\mathrm{lj}}^2 = N\mu_2 \\ \sum_{l=1}^{N} x_{\mathrm{lj}}^4 = 3\sum_{l=1}^{N} x_{\mathrm{lk}}^2 x_{\mathrm{lj}}^2 = 3N\mu_4 \\ \sum_{l=1}^{N} x_{\mathrm{lj}}^6 = 5\sum_{l=1}^{N} x_{\mathrm{lk}}^4 x_{\mathrm{lj}}^2 = 15N\mu_6 \\ k, j = 1, 2\ (k \neq j) \end{cases} \tag{8}$$

where μ_2, μ_4, and μ_6 represent the regressive parameters.

It can be seen from (8) that the regressive parameters μ_2, μ_4, and μ_6 depend only on the regressor values of the given points. In other words, μ_2, μ_4, and μ_6 can be computed from (8) as soon as all the given points are determined.

Substituting (7) and (8) into (6) results in

$$\boldsymbol{A} = \begin{pmatrix} \boldsymbol{G} & \boldsymbol{Z}_2 & \boldsymbol{Z}_3 & \boldsymbol{Z}_3 \\ \boldsymbol{Z}_1 & N\mu_4 & \boldsymbol{Z}_1 & \boldsymbol{Z}_1 \\ \boldsymbol{Z}_3 & \boldsymbol{Z}_2 & \boldsymbol{H} & \boldsymbol{Z}_3 \\ \boldsymbol{Z}_3 & \boldsymbol{Z}_2 & \boldsymbol{Z}_3 & \boldsymbol{H} \end{pmatrix} \tag{9}$$

where

$$\boldsymbol{G} = \begin{pmatrix} N & N\mu_2 & N\mu_2 \\ N\mu_2 & 3N\mu_4 & N\mu_4 \\ N\mu_2 & N\mu_4 & 3N\mu_4 \end{pmatrix} \tag{10}$$

$$\boldsymbol{H} = \begin{pmatrix} N\mu_2 & 3N\mu_4 & N\mu_4 \\ 3N\mu_4 & 15N\mu_6 & 3N\mu_6 \\ N\mu_4 & 3N\mu_6 & 3N\mu_6 \end{pmatrix} \tag{11}$$

and

$$\boldsymbol{Z}_1 = (0 \quad 0 \quad 0), \quad \boldsymbol{Z}_2 = \begin{pmatrix} 0 \\ 0 \\ 0 \end{pmatrix}, \quad \boldsymbol{Z}_3 = \begin{pmatrix} 0 & 0 & 0 \\ 0 & 0 & 0 \\ 0 & 0 & 0 \end{pmatrix}. \tag{12}$$

Consequently, the inverse matrix of $\boldsymbol{A}$ can be determined by

$$\boldsymbol{A}^{-1} = \begin{pmatrix} \boldsymbol{G}^{-1} & \boldsymbol{Z}_2 & \boldsymbol{Z}_3 & \boldsymbol{Z}_3 \\ \boldsymbol{Z}_1 & (N\mu_4)^{-1} & \boldsymbol{Z}_1 & \boldsymbol{Z}_1 \\ \boldsymbol{Z}_3 & \boldsymbol{Z}_2 & \boldsymbol{H}^{-1} & \boldsymbol{Z}_3 \\ \boldsymbol{Z}_3 & \boldsymbol{Z}_2 & \boldsymbol{Z}_3 & \boldsymbol{H}^{-1} \end{pmatrix} \tag{13}$$

where $\boldsymbol{G}^{-1}$ and $\boldsymbol{H}^{-1}$ are, respectively, expressed as

$$\boldsymbol{G}^{-1} = \begin{pmatrix} g_{11} & g_{12} & g_{13} \\ g_{21} & g_{22} & g_{23} \\ g_{31} & g_{32} & g_{33} \end{pmatrix} \tag{14}$$

and

$$\boldsymbol{H}^{-1} = \begin{pmatrix} h_{11} & h_{12} & h_{13} \\ h_{21} & h_{22} & h_{23} \\ h_{31} & h_{32} & h_{33} \end{pmatrix}. \tag{15}$$

Based on the regression technique [8], the coefficients matrix $\boldsymbol{R}$ in (1) can be determined by

$$\boldsymbol{R} = (\boldsymbol{Y}^t \boldsymbol{Y})^{-1} (\boldsymbol{Y}^t \boldsymbol{T}_g) = \boldsymbol{A}^{-1} \boldsymbol{B} \tag{16}$$

$$\boldsymbol{Y} = \begin{pmatrix} 1 & x_{11}^2 & x_{12}^2 & x_{11}x_{12} & x_{11} & x_{11}^3 & x_{11}x_{12}^2 & x_{12} & x_{12}^3 & x_{11}^2 x_{12} \\ 1 & x_{21}^2 & x_{22}^2 & x_{21}x_{22} & x_{21} & x_{21}^3 & x_{21}x_{22}^2 & x_{22} & x_{22}^3 & x_{21}^2 x_{22} \\ \vdots & \vdots & \vdots & \vdots & \vdots & \vdots & \vdots & \vdots & \vdots & \vdots \\ 1 & x_{l1}^2 & x_{l2}^2 & x_{l1}x_{l2} & x_{l1} & x_{l1}^3 & x_{l1}x_{l2}^2 & x_{l2} & x_{l2}^3 & x_{l1}^2 x_{l2} \\ \vdots & \vdots & \vdots & \vdots & \vdots & \vdots & \vdots & \vdots & \vdots & \vdots \\ 1 & x_{N1}^2 & x_{N2}^2 & x_{N1}x_{N2} & x_{N1} & x_{N1}^3 & x_{N1}x_{N2}^2 & x_{N2} & x_{N2}^3 & x_{N1}^2 x_{N2} \end{pmatrix}. \tag{7}$$

where $\boldsymbol{T}_g$ represents the given torque matrix corresponding to the given points, which is expressed by

$$\boldsymbol{T}_g = \begin{pmatrix} T_{1g} \\ T_{2g} \\ \vdots \\ T_{lg} \\ \vdots \\ T_{\mathrm{Ng}} \end{pmatrix}. \tag{17}$$

$\boldsymbol{B}$ is computed from

$$\boldsymbol{B} = \boldsymbol{Y}^t \boldsymbol{T}_g = \begin{pmatrix} \sum_{l=1}^{N} T_{lg} \\ \sum_{l=1}^{N} x_{l1}^2 T_{lg} \\ \sum_{l=1}^{N} x_{l2}^2 T_{lg} \\ \sum_{l=1}^{N} x_{l1} x_{l2} T_{lg} \\ \sum_{l=1}^{N} x_{l1} T_{lg} \\ \sum_{l=1}^{N} x_{l1}^3 T_{lg} \\ \sum_{l=1}^{N} x_{l1} x_{l2}^2 T_{lg} \\ \sum_{l=1}^{N} x_{l2} T_{lg} \\ \sum_{l=1}^{N} x_{l2}^3 T_{lg} \\ \sum_{l=1}^{N} x_{l1}^2 x_{l2} T_{lg} \end{pmatrix}. \tag{18}$$

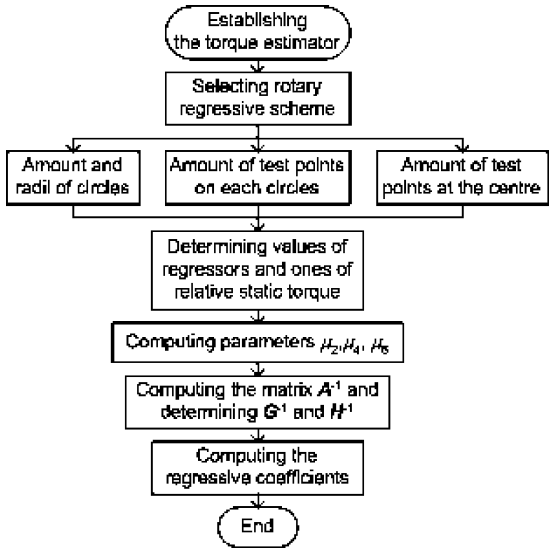

Fig. 2. Flowchart for computing the regressive coefficients.

By substituting (13) and (18) into (16), one can have (19). Note that (19) may be computed offline or online. As a result, the instantaneous torque at an arbitrary rotor position and current can be estimated from (1) in real time. Fig. 2 illustrates the flowchart to compute the regressive coefficients.

C. Torque in SRM Drives

In general, the mutual coupling between phases in SRM drives is neglected in the design of torque ripple minimization algorithm. However, the effect of mutual coupling does exist [9], and it is not negligible. During phase commutation, the effect

$$\boldsymbol{R} = \begin{pmatrix} g_{11}\sum_{l=1}^{N} T_{lg} + g_{12}\sum_{l=1}^{N} x_{l1}^2 T_{lg} + g_{13}\sum_{l=1}^{N} x_{l2}^2 T_{lg} \\ g_{21}\sum_{l=1}^{N} T_{lg} + g_{22}\sum_{l=1}^{N} x_{l1}^2 T_{lg} + g_{23}\sum_{l=1}^{N} x_{l2}^2 T_{lg} \\ g_{31}\sum_{l=1}^{N} T_{lg} + g_{32}\sum_{l=1}^{N} x_{l1}^2 T_{lg} + g_{33}\sum_{l=1}^{N} x_{l2}^2 T_{lg} \\ (N\mu_4)^{-1}\sum_{l=1}^{N} x_{l1} x_{l2} T_{lg} \\ h_{11}\sum_{l=1}^{N} x_{l1} T_{lg} + h_{12}\sum_{l=1}^{N} x_{l1}^3 T_{lg} + h_{13}\sum_{l=1}^{N} x_{l1} x_{l2}^2 T_{lg} \\ h_{21}\sum_{l=1}^{N} x_{l1} T_{lg} + h_{22}\sum_{l=1}^{N} x_{l1}^3 T_{lg} + h_{23}\sum_{l=1}^{N} x_{l1} x_{l2}^2 T_{lg} \\ h_{31}\sum_{l=1}^{N} x_{l1} T_{lg} + h_{32}\sum_{l=1}^{N} x_{l1}^3 T_{lg} + h_{33}\sum_{l=1}^{N} x_{l1} x_{l2}^2 T_{lg} \\ h_{11}\sum_{l=1}^{N} x_{l2} T_{lg} + h_{12}\sum_{l=1}^{N} x_{l2}^3 T_{lg} + h_{13}\sum_{l=1}^{N} x_{l1}^2 x_{l2} T_{lg} \\ h_{21}\sum_{l=1}^{N} x_{l2} T_{lg} + h_{22}\sum_{l=1}^{N} x_{l2}^3 T_{lg} + h_{23}\sum_{l=1}^{N} x_{l1}^2 x_{l2} T_{lg} \\ h_{31}\sum_{l=1}^{N} x_{l2} T_{lg} + h_{32}\sum_{l=1}^{N} x_{l2}^3 T_{lg} + h_{33}\sum_{l=1}^{N} x_{l1}^2 x_{l2} T_{lg} \end{pmatrix}. \tag{19}$$

of the mutual coupling between the adjacent phases must, indeed, be taken into consideration in order to obtain an accurate estimation of the motor torque.

Taking into account the mutual coupling in SRM drives, the instantaneous torque generated by one phase is composed of two components as expressed in [9]:

$$T_k = T_{ks} + T_{km} \tag{20}$$

where T_k represents the instantaneous torque from phase k, T_{ks} represents the instantaneous self-coupling torque generated by the current in phase k, and T_{km} represents the instantaneous mutual-coupling torque generated by the current in the phase adjacent to phase k.

The torque from phase k is the self-coupling torque produced by the current in phase k if the mutual coupling is neglected. The self-coupling torque characteristics with respect to the position and current are the same as the static torque characteristics of SRM drives. Such characteristics can be measured directly by means of a torque sensor. They can also be acquired indirectly based on the flux linkage characteristics with respect to the rotor position and current. If the flux linkage characteristics are obtained experimentally, the self-coupling torque generated by phase k can be computed from

$$W'_{kk}(\theta, i_k) = \int_0^{i_k} \psi_{kk}(\theta, i)\, di \tag{21}$$

$$T_{ks}(\theta, i_k) = \frac{\partial W'_{kk}(\theta, i_k)}{\partial \theta} \tag{22}$$

where W'_{kk} denotes the self-coupling co-energy generated by phase k, ψ_{kk} denotes the given self-coupling flux linkage characteristics, and i_k denotes the current in phase k.

The mutual-coupling torque needs to be experimentally measured indirectly via the mutual-coupling flux linkage characteristics. If the mutual-coupling flux linkage characteristics are given, the mutual-coupling torque can be determined by

$$W'_{kj}(\theta, i_j) = \int_0^{i_j} \psi_{kj}(\theta, i)\, di \tag{23}$$

$$T_{km}(\theta, i_j) = \frac{\partial W'_{kj}(\theta, i_j)}{\partial \theta} \tag{24}$$

where W'_{kj} denotes the mutual-coupling co-energy in phase k, which is generated by phase j adjacent to phase k, ψ_{kj} denotes the given mutual-coupling flux linkage in phase k, which is generated by phase j adjacent to phase k, and i_j denotes the current in phase j.

III. Applications

A prototype of the four-phase SRM drive is used to validate the proposed torque estimator. Because both the self-coupling and mutual-coupling torque characteristics are highly nonlinear, and the proposed torque estimator consists of a bicubic regressive polynomial, the given torque characteristics are divided into four regimes in order to enhance the accuracy of the torque estimator.

1) $\theta_{\min 1} \le \theta \le \theta_{\max 1}$ and $i_{\min 1} \le i \le i_{\max 1}$,
2) $\theta_{\min 2} \le \theta \le \theta_{\max 2}$ and $i_{\min 1} \le i \le i_{\max 1}$,
3) $\theta_{\min 1} \le \theta \le \theta_{\max 1}$ and $i_{\min 2} \le i \le i_{\max 2}$,
4) $\theta_{\min 2} \le \theta \le \theta_{\max 2}$ and $i_{\min 2} \le i \le i_{\max 2}$.

In this study, the rotor position is equal to 0° when the stator pole is just unaligned with the rotor pole, and the rotor position is equal to 30° when the stator pole is just aligned with the rotor pole. The rotary regression schemes for the aforementioned various parts are the same. It can be found from (2) that the proposed torque estimator within each part requires 10 regressive coefficients. Thus, 40 regressive coefficients are to be determined and stored for the self-coupling or mutual-coupling torque characteristics. The developed rotary regression scheme is described as follows: four circles are selected and their radii are $\rho_1 = 1.0$, $\rho_2 = 0.9$, $\rho_3 = 0.7$, and $\rho_4 = 0.5$. A total of 64 given points are distributed symmetrically on each circle, and there are four given points on the center.

A. Self-Coupling Torque Estimator

The self-coupling torque characteristics of SRM drives are the same as their static torque characteristics. For four-phase SRM drives, the period of the static torque characteristics is 60 mechanical degrees, and the static torque characteristics are antisymmetrical about the position of 30°. Hence, the positions ranging from 0° to 30° are selected as the domain of the rotor position for the self-coupling torque estimator. The parameters of four parts are selected as $\theta_{\min 1} = 0^\circ$, $\theta_{\max 1} = 7.5^\circ$, $\theta_{\min 2} = 7.5^\circ$, $\theta_{\max 2} = 30^\circ$, $i_{\min 1} = 0\text{A}$, $i_{\max 1} = 3\text{A}$, $i_{\min 2} = 3\text{A}$, and $i_{\max 2} = 12\text{A}$. Furthermore, for the static torque characteristics of the prototype, the proposed self-coupling torque estimator should satisfy the constraint such that the self-coupling torque must be zero when the current is equal to zero, the rotor position is equal to 30°, and the rotor position is greater than 0° and smaller than 2°. Indeed, the torque is theoretically zero at 0° and 30°. The experimental and computed results from the prototype show that the torque is approximately zero within the range from 0° to 2°.

Table I shows the computed regressive coefficients in the first regime ($\theta_{\min 1} \le \theta \le \theta_{\max 1}$ and $i_{\min 1} \le i \le i_{\max 1}$) and the second regime ($\theta_{\min 2} \le \theta \le \theta_{\max 2}$ and $i_{\min 1} \le i \le i_{\max 1}$), respectively. Table II lists the computed regressive coefficients in the third regime ($\theta_{\min 1} \le \theta \le \theta_{\max 1}$ and $i_{\min 2} \le i \le i_{\max 2}$) and the fourth regime ($\theta_{\min 2} \le \theta \le \theta_{\max 2}$ and $i_{\min 2} < i \le i_{\max 2}$), respectively.

Fig. 3 illustrates the estimated self-coupling torque values from the proposed self-coupling torque estimator and the experimental values. It can be observed that the estimated torque values are, generally, very close to the given values. Hence, the proposed self-coupling torque estimator is accurate.

B. Mutual-Coupling Torque Estimator

In this paper, the mutual coupling between adjacent phases is taken into account. For the prototype of the four-phase SRM drive, the mutual-coupling torque T_{ad} and T_{ab} for phase A,

TABLE I
REGRESSIVE COEFFICIENTS IN THE FIRST AND SECOND REGIMES FOR THE SELF-COUPLING TORQUE ESTIMATOR

Coefficients	First part	Second part
r_0	.127340E+00	.744259E+00
r_1	.389936E+00	-.504969E-01
r_2	.219412E+00	.137407E+01
r_{12}	.665176E+00	-.248222E+00
r_{11}	.196639E+00	-.629561E+00
r_{22}	.117300E+00	.533139E+00
r_{122}	.318928E+00	-.162318E+00
r_{211}	.476047E+00	-.910323E+00
r_{111}	-.139924E+00	-.145043E+00
r_{222}	-.152754E-01	-.740014E-01

TABLE II
REGRESSIVE COEFFICIENTS IN THE THIRD AND FOURTH REGIMES FOR THE SELF-COUPLING TORQUE ESTIMATOR

Coefficients	Third part	Fourth part
r_0	.107503E+01	.503973E+01
r_1	.286642E+01	-.125834E+01
r_2	.170675E+01	.643300E+01
r_{12}	.362531E+01	-.245969E+01
r_{11}	.117034E+01	-.383915E+01
r_{22}	.577029E+00	.440465E+00
r_{122}	.115784E+01	-.113415E+01
r_{211}	.161459E+01	-.433218E+01
r_{111}	-.924871E+00	-.123519E+00
r_{222}	-.140974E+00	-.911735E+00

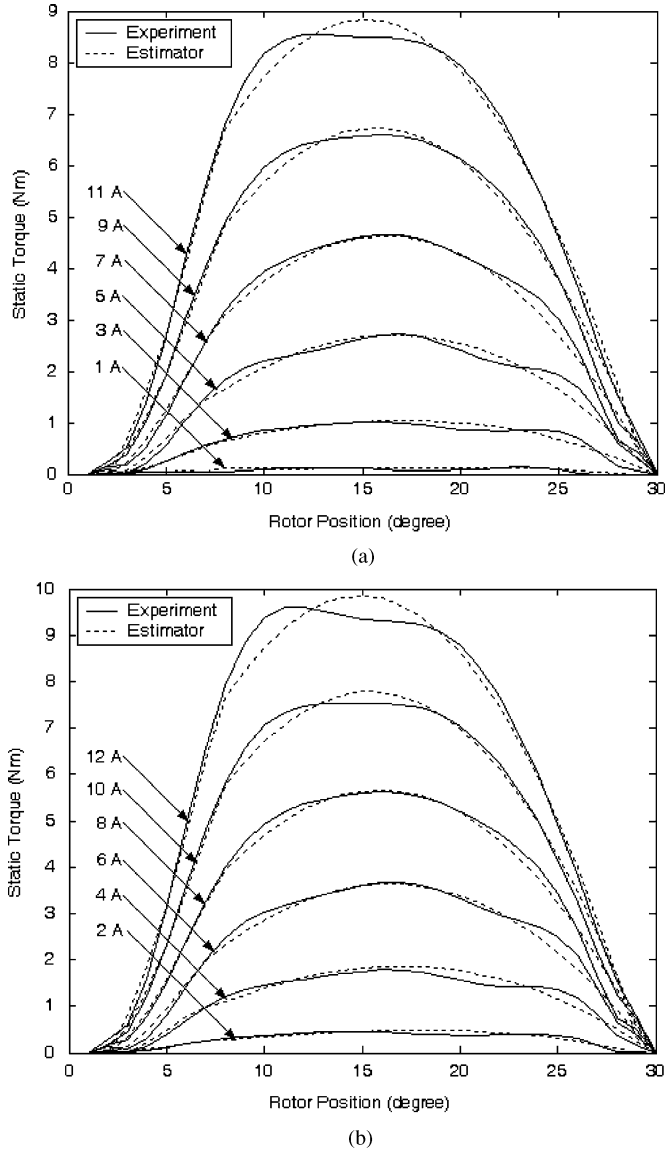

Fig. 3. Experimental and estimated self-coupling torque characteristics.

generated by the current in phase D and the current in phase B, can be represented approximately by the profiles shown in Fig. 4, if phase A is selected as the reference phase.

Clearly, the period of the mutual-coupling torque characteristics is also 60° for four-phase SRM drives. It can be observed from Fig. 4 that the mutual-coupling torque characteristics $(T_{\rm ad})$ for phase A, which is generated by the current in phase D, are antisymmetrical about the position of 20°. $T_{\rm ad}$ is zero within the position range from 40° to 60°. Similarly, $T_{\rm ab}$ is inverse symmetrical about the position of 40°, and is zero within the positions ranging from 0° to 20°. If the mutual-coupling torque characteristics (T_m) in the positions ranging from 0° to 20° are given, the mutual-coupling torque values ($T_{\rm ad}$ and $T_{\rm ab}$) at any position and current can be computed from

$$T_{\rm ad}(\theta,i)=\begin{cases} T_m(\theta,i), & 0\le\theta\le 20\\ -T_m(40-\theta,i), & 20\le\theta\le 40\\ 0, & 40\le\theta\le 60\end{cases} \tag{25}$$

and

$$T_{\rm ab}(\theta,i)=-T_{\rm ad}(60-\theta,i). \tag{26}$$

Hence, the given mutual-coupling characteristics (T_m) can be used to determine the mutual-coupling torque estimator. The rotary regression scheme for the mutual-coupling torque estimator is the same as the one for the self-coupling torque estimator. The parameters of four regimes for the mutual-coupling torque estimator are selected as $\theta_{\rm min1}=0°$, $\theta_{\rm max1}=8.5°$, $\theta_{\rm min2}=8.5°$, $\theta_{\rm max2}=20°$, $i_{\rm min1}=0$A, $i_{\rm max1}=3$A, $i_{\rm min2}=3$A, and $i_{\rm max2}=12$A. The computed regressive coefficients for the mutual-coupling torque estimator are shown in Tables III and IV.

The comparisons between the estimated and given mutual-coupling torque characteristics are illustrated in Fig. 5. It is clear that the estimated and the given values are in good agreement. Therefore, the proposed mutual-coupling torque estimator can be used to accurately compute the mutual-coupling torque.

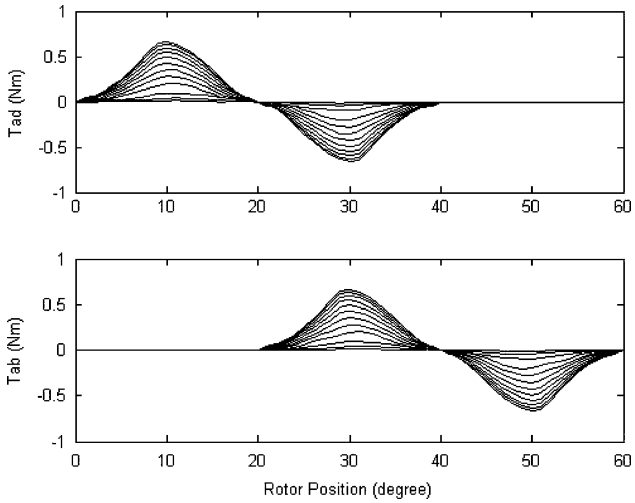

Fig. 4. Mutual-coupling torque characteristics generated by the adjacent phases for the four-phase SRM drive.

TABLE III
REGRESSIVE COEFFICIENTS IN THE FIRST AND SECOND PARTS FOR THE MUTUAL-COUPLING TORQUE ESTIMATOR

Coefficients	First part	Second part
r_0	.154219E-01	.528912E-01
r_1	.338922E-01	-.556254E-01
r_2	.361986E-01	.105757E+00
r_{12}	.750078E-01	-.813795E-01
r_{11}	.222712E-01	-.379414E-01
r_{22}	.279171E-01	.434052E-01
r_{122}	.450344E-01	-.547235E-01
r_{211}	.476528E-01	-.643275E-01
r_{111}	-.126526E-02	.485029E-01
r_{222}	.251352E-02	-.870452E-02

TABLE IV
REGRESSIVE COEFFICIENTS IN THE THIRD AND FOURTH PARTS FOR THE MUTUAL-COUPLING TORQUE ESTIMATOR

Coefficients	Third part	Fourth part
r_0	.165119E+00	.326829E+00
r_1	.305732E+00	-.413526E+00
r_2	.181800E+00	.316655E+00
r_{12}	.247245E+00	-.265057E+00
r_{11}	.887253E-01	-.162103E+00
r_{22}	-.500527E-01	-.866426E-01
r_{122}	-.937960E-01	.116095E+00
r_{211}	.922963E-01	-.130263E+00
r_{111}	-.818615E-01	.280465E+00
r_{222}	-.543926E-01	-.665773E-01

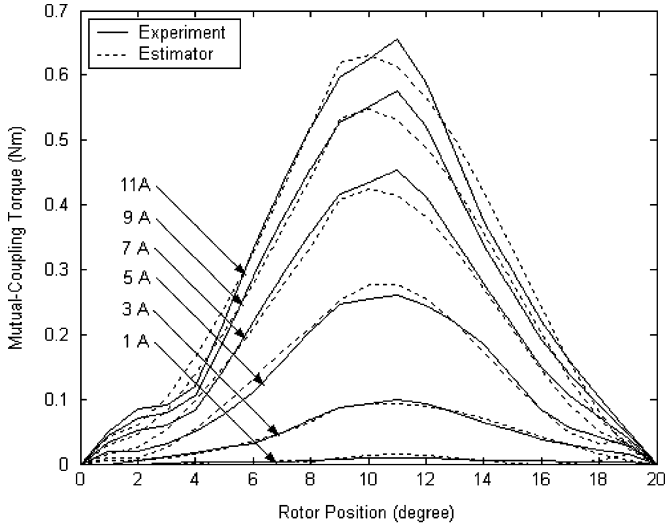

(a)

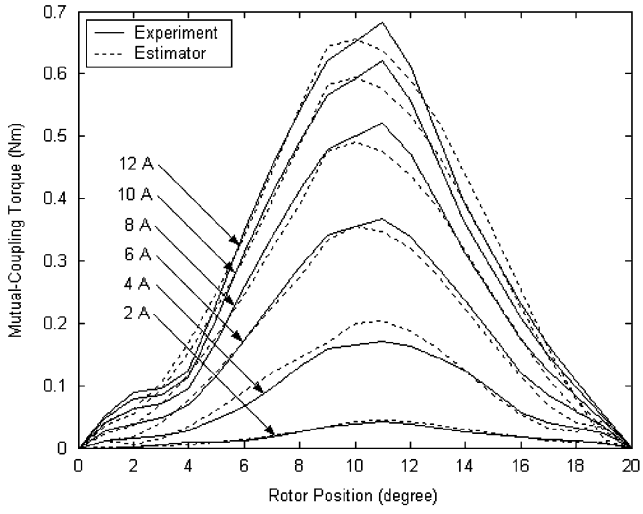

(b)

Fig. 5. Experimental and estimated mutual-coupling torque characteristics.

C. Dynamic Torque Estimation

To examine the proposed self-coupling and mutual-coupling torque estimators, they are used to estimate the dynamic torque in real time and the dynamic torque waveforms under three controls are simulated using the proposed torque estimators. Firstly, the mutual coupling is neglected, and only the dynamic torque without the mutual-coupling is taken into account. Fig. 6(b) shows the dynamic self-coupling torque waveforms from the bicubic spline interpolation [10] and the proposed self-coupling torque estimator with single-pulse voltage control. Both torque waveforms are produced by the same phase current profile, as shown in Fig. 6(a). In the same way, the dynamic self-coupling torque waveforms with hysteresis current chopping control and voltage pulse width modulation (PWM) control are depicted in Figs. 7 and 8, respectively. It can be seen that the dynamic self-coupling torque waveforms estimated by the proposed torque estimator are in good agreement with those obtained from the bicubic spline interpolation with these three controls, as mentioned earlier.

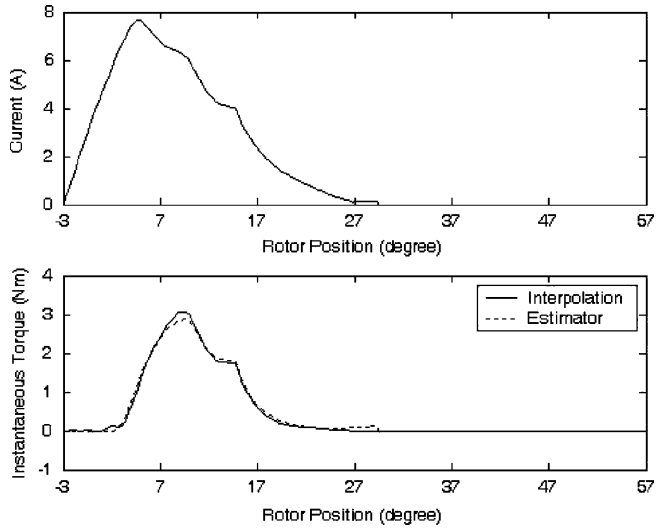

Fig. 6. Interpolated and estimated dynamic phase torque waveforms without considering the mutual-coupling with single-pulse voltage control.

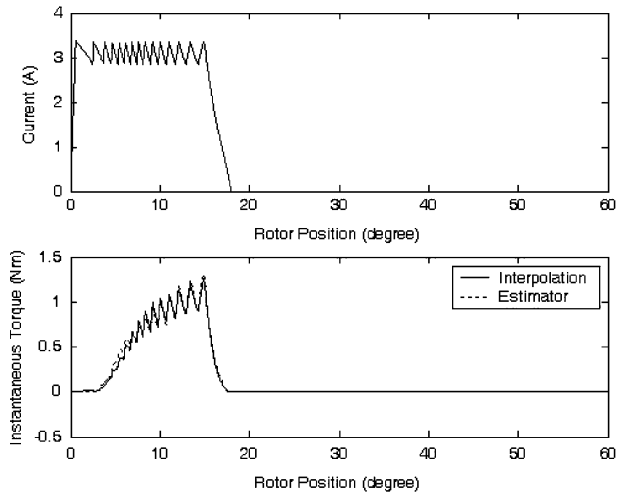

Fig. 7. Interpolated and estimated dynamic phase torque waveforms without considering the mutual coupling with hysteresis current chopping control.

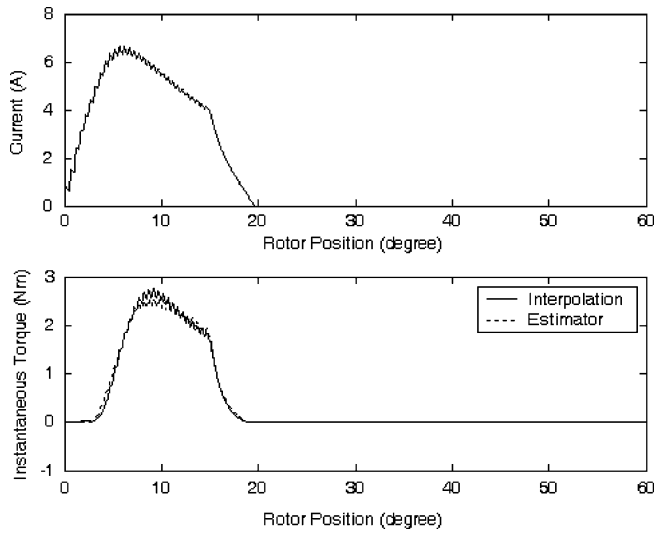

Fig. 8. Interpolated and estimated dynamic phase torque waveforms without considering the mutual-coupling with voltage PWM control.

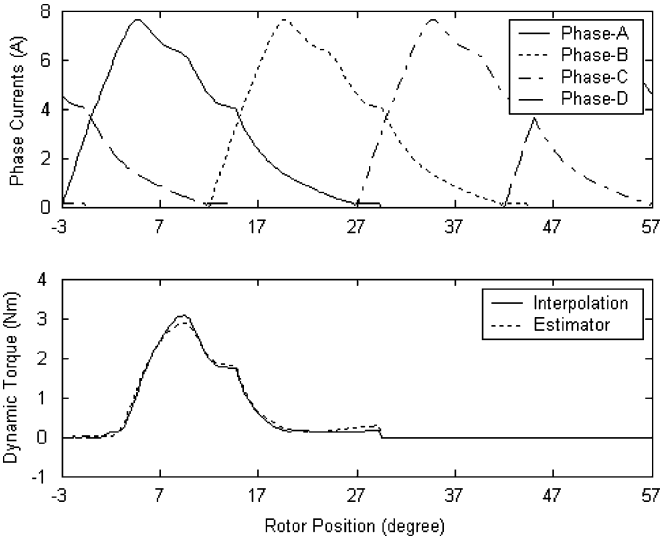

Fig. 9. Interpolated and estimated dynamic phase torque waveforms with the inclusion of mutual-coupling with single-pulse voltage control.

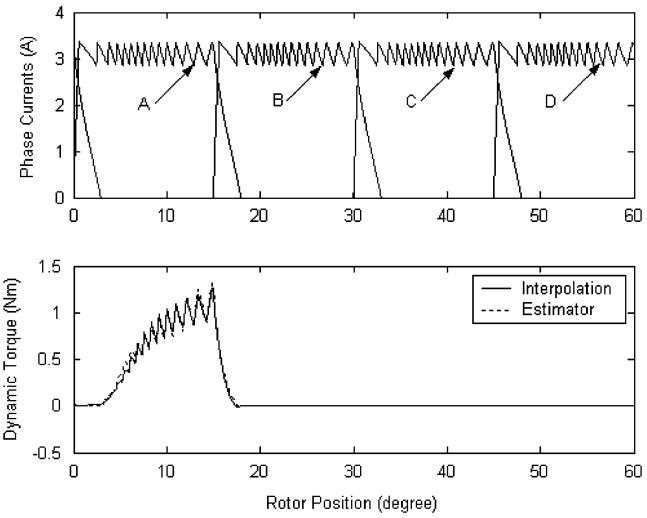

Fig. 10. Interpolated and estimated dynamic phase torque waveforms with the inclusion of mutual-coupling with hysteresis current chopping control.

Then, both the self-coupling torque and mutual-coupling torque are considered. In other words, the proposed self-coupling and mutual-coupling torque estimators are used to estimate the dynamic torque by taking mutual coupling into consideration. Figs. 9–11 depict the dynamic phase torque profiles generated by the self-coupling and mutual-coupling phase currents with single-pulse voltage, hysteresis current chopping, and voltage PWM control modes, respectively. It can be seen that the dynamic phase torque profiles estimated by the proposed self-coupling and mutual-coupling torque estimators are in good agreement with the predicted ones using the bicubic spline interpolation.

Clearly, not only the comparisons between the estimated and given self-coupling and mutual-coupling torque characteristics, but also the dynamic torque profiles from the proposed estimators and the bicubic spline interpolation, can demonstrate that

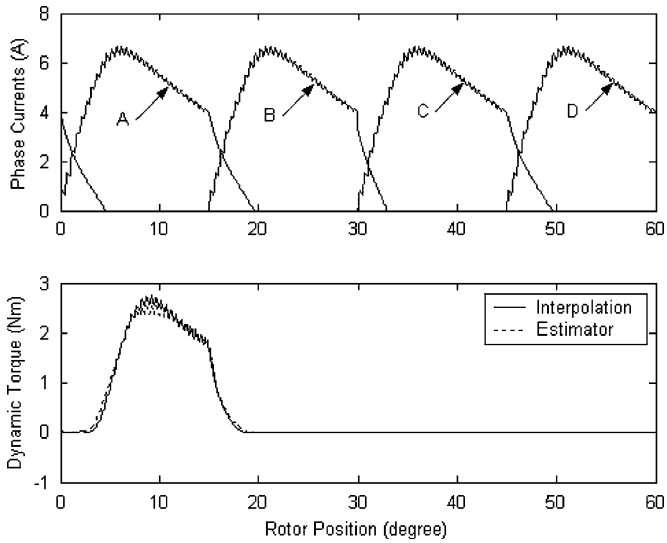

Fig. 11. Interpolated and estimated dynamic phase torque waveforms with the inclusion of mutual-coupling with the voltage PWM control.

the developed self-coupling and mutual-coupling torque estimators are accurate. In summary, the proposed torque estimator, which consists of a simple bicubic polynomial that requires a very small amount of stored data, can be used to accurately and quickly estimate the static or dynamic torque of an SRM drive with or without the inclusion of mutual coupling.

IV. Conclusion

A new torque estimator based on the rotary regression analysis has been developed in this paper. The proposed torque estimator consists only of a bicubic regressive polynomial with respect to rotor position and motor current. The regressive coefficients in the estimator can be computed offline or online from predetermined torque characteristics acquired by experiment or numerical computation. Moreover, a torque-estimation method with the inclusion of mutual coupling has been proposed. The estimated and given self-coupling and mutual-coupling torque characteristics are in good agreement. Furthermore, the estimated dynamic torque waveforms with and without the mutual coupling are found to be in good agreement with those obtained from the bicubic spline interpolation. Overall, the case studies as reported in this paper are a good demonstration of the usefulness of the proposed self-coupling and mutual-coupling torque estimators.

By using the rotary regression technique as proposed, the torque estimator needs to store a small number of coefficients and execute simple computation only. Hence, the salient advantages of the proposed torque estimator are the rapidity of the computation and the need for very minimal computer memories. In summary, this paper provides a valuable approach to rapidly estimate the instantaneous torque of SRM drives in real time.

References

[1] I. Husain, "Minimization of torque ripple in SRM drives," *IEEE Trans. Ind. Electron.*, vol. 49, no. 1, pp. 28–39, Feb. 2002.

[2] J. Corda, S. Masic, and J. M. Stephenson, "Computation and experimental determination of running torque waveforms in switched-reluctance motors," *Inst. Electr. Eng. Proc. B*, vol. 140, no. 6, pp. 387–392, Nov. 1993.

[3] J. C. Moreira, "Torque ripple minimization in switched reluctance motors via bi-cubic spline interpolation," in *in Proc. 23rd Annu. IEEE Power Electron. Specialists Conf. (PESC'92)*, 1992, vol. 2, pp. 851–856.

[4] K. Russa, I. Husain, and M. E. Elbuluk, "Torque-ripple minimization in switched reluctance machines over a wide speed range," *IEEE Trans. Ind. Appl.*, vol. 34, no. 5, pp. 1105–1112, Sep. 1998.

[5] N. C. Sahoo, J. X. Xu, and S. K. Panda, "Determination of current waveforms for torque ripple minimization in switched reluctance motors using iterative learning: An investigation," *Inst. Electr. Eng. Proc. Electr. Power Appl.*, vol. 146, no. 4, pp. 369–377, Jul. 1999.

[6] S. K. Sahoo, Q. Zheng, S. K. Panda, and J. X. Xu, "Model-based torque estimator for switched reluctance motors," in *Proc. 5th Int. Conf. Power Electron. Drive Syst. 2003 (PEDS 2003)*, vol. 2, Nov. 17–20, pp. 959–963.

[7] B. Fahimi, G. Suresh, and M. Ehsani, "Torque estimation in switched reluctance motor drive using artificial neural networks," in *Proc. 23rd Int. Conf. Ind. Electron., Control Instrum. (IECON'97)*, vol. 1, 1997, pp. 21–26.

[8] S. S. Mao, Y. Ding, J. X. Zhou, and N. G. Lü, *Regression Analysis and Its Test Schemes*. Shanghai, China: East China Normal Univ., 1986.

[9] X. D. Xue, K. W. E. Cheng, and S. L. Ho, "An algorithm for solving value problems of multiphase switched reluctance motors taking account of mutual coupling," *Electr. Power Component Syst.*, vol. 30, pp. 637–651, 2002.

[10] X. D. Xue, K. W. E. Cheng, and S. L. Ho, "Simulation of switched reluctance motor drives using two-dimensional bicubic spline," *IEEE Trans. Energy Convers.*, vol. 17, no. 4, pp. 471–477, Dec. 2002.

X. D. Xue received the Bachelor's degree from Hefei University of Technology, Hefei, China, in 1984, the Master's degree from Tianjin University, Tianjin, China, in 1987, and the Ph.D. degree from the Hong Kong Polytechnic University, kowloon, Hong Kong, in 2004, all in electrical engineering.

From 1987 to 2001, he was engaged in teaching and research in the Department of Electrical Engineering, Tianjin University. He is currently with the Department of Electrical Engineering, Hong Kong Polytechnic University. His current research interests include electrical machines, electrical drives, and power electronics.

K. W. E. Cheng (M'90–SM'06) received the B.Sc. and Ph.D. degrees in electrical engineering from the University of Bath, Bath, U.K., in 1987 and 1990, respectively.

He was a Principal Engineer with Lucas Aerospace, Birmingham, U.K., where he led a number of power electronics projects. In 1997, he joined the Hong Kong Polytechnic University, Kowloon, Hong Kong, where he is currently a Professor and the Director of the Power Electronics Research Centre. His current research interests include all aspects of power electronics. He is the author or coauthor of more than 200 published papers and seven books.

Prof. Cheng received the Institution of Electrical Engineering (IEE) Sebastian Z De Ferranti Premium Award in 1995, the Outstanding Consultancy Award in 2000, the Faculty Merit Award for Best Teaching in 2003, and the Research and Scholarly Activities Award from the Hong Kong Polytechnic University in 2006.

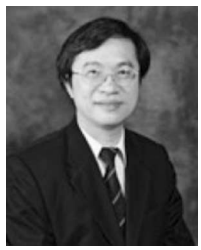

S. L. Ho received the B.Sc. and Ph.D. degrees in electrical engineering from the University of Warwick, Coventry, U.K., in 1976 and 1979, respectively.

In 1979, he joined the Hong Kong Polytechnic University, Kowloon, Hong Kong, where he is currently the Chair Professor of electrical utilization and the Head of the Department of Electrical Engineering. He has been engaged in the local industry, particularly in railway engineering. He is the holder of several patents, and is the author or coauthor of more than 100 papers published in leading journals, mostly in the IEEE Transactions and the *Institution of Electrical Engineering Proceedings*. His current research interests include traction engineering, application of finite elements in electrical machines, phantom loading of machines, and optimization of electromagnetic devices.

Prof. Ho is a member of the Institution of Electrical Engineers, U.K., and the Hong Kong Institution of Engineers.